# Characterizing steady-state and transient properties of reaction-diffusion systems

Sven Dorosz and Michel Pleimling
*Department of Physics, Virginia Polytechnic Institute and State University, Blacksburg, Virginia 24061-0435, USA*
(Received 2 October 2009; published 14 December 2009)

In the past, the study of reaction-diffusion systems has greatly contributed to our understanding of the behavior of many-body systems far from equilibrium. In this paper, we aim at characterizing the properties of diffusion-limited reactions both in their steady states and out of stationarity. Many reaction-diffusion systems have the peculiarity that microscopic reversibility is broken such that their transient behavior cannot be investigated through the study of most of the observables discussed in the literature. For this reason, we analyze the transient properties of reaction-diffusion systems through a specific work observable that remains well defined even in the absence of microscopic reversibility and that obeys an exact detailed fluctuation relation in cases where detailed balance is fulfilled. We thereby drive the systems out of their nonequilibrium steady states through time-dependent reaction rates. Using a numerical exact method and computer simulations, we analyze fluctuation ratios of the probability distributions obtained during the forward and reversed processes. We show that the underlying microscopic dynamics gives rise to peculiarities in the configuration-space trajectories, thereby, yielding prominent features in the fluctuation ratios.

DOI: 10.1103/PhysRevE.80.061114 PACS number(s): 05.40.−a, 05.70.Ln, 05.20.−y

## I. INTRODUCTION

Understanding general properties of systems that are far from equilibrium remains one of the most challenging problems in contemporary physics. In recent years, some remarkable progress has been made in the study of fluctuations in nonequilibrium small systems (see, e.g., [1–24]). This progress is mainly due to the formulation of various exact fluctuation and work theorems that provide very generic statements that hold true for large classes of systems. Some of the fluctuation theorems deal with the rate of entropy production, either in systems that are in a nonequilibrium steady state [2,3] or in systems that initially are in equilibrium before being driven out of equilibrium by an external force [6,8]. One also distinguishes between detailed [9,11,14] and integral [4,12,15] fluctuation theorems in cases where the system is driven from one steady state to another in finite time. In addition, work theorems [4,5,9] relate the free-energy difference between two equilibrium states to the amount of work done during the switching from one state to the other. Many of these theorems have been verified in various experimental settings [17–24], thus, illustrating their usefulness for characterizing nonequilibrium systems.

In the past, diffusion-limited reaction systems have been proven to be extremely useful in order to understand the generic behavior of many-body systems far from equilibrium. Especially, the study of these systems is at the origin of our understanding of the properties of nonequilibrium phase transitions [25,26]. Whereas phase transitions in reaction-diffusion systems are by now very well characterized, this is quite different away from these special points. In the present work, we discuss different ways of characterizing the steady-state and transient properties of generic reaction-diffusion systems, thus, contributing to a more comprehensive understanding of these important systems.

Recently, discussed extensions of exact fluctuation theorems to nonequilibrium systems with chemical reactions mostly focused on reversible reactions and reaction networks [27–33]. However, many reaction-diffusion models are characterized by *irreversible* reactions, thus, yielding a breaking of the usually assumed microscopic reversibility. By breaking microscopic reversibility, we mean that if $\omega(C_i \to C_j)$ is the transition probability from configuration $C_i$ to configuration $C_j$, it can happen that $\omega(C_i \to C_j)=0$ even though $\omega(C_j \to C_i) > 0$. A direct consequence of the absence of microscopic reversibility is that many observables discussed in the context of fluctuation theorems are then ill defined, as in their derivation one explicitly uses that for any path in configuration space the reversed path also exists [34,35]. For this reason, we focus in our study of fluctuations in reaction-diffusion systems on an observable that is well defined even in the absence of microscopic reversibility. For a system initially in an equilibrium steady state, this quantity is identical to the work observable used in the Jarzynski and Crooks relations [4,5,10].

It should be noted that diffusion-limited systems with effective irreversible reactions can be prepared through a fast evacuation of some of the reaction products. This makes plausible a possible future verification of the intriguing features that are revealed in our study.

In the following, we discuss, using a numerical exact method and numerical simulations, steady-state and transient properties of various reaction-diffusion systems. Especially, we study fluctuations in systems that are initially in a steady state before being driven away from stationarity by varying one of the reaction rates. This protocol allows us to measure the probability distribution (PD) of our observable when going from a steady state $A$, characterized by the value $r_A$ of some reaction rate $r$, to another steady state $B$, characterized by the value $r_B$ of the same reaction rate. Defining the reversed process as changing the reaction rate backward from $r_B$ to $r_A$, we can measure also the probability distribution in that case and compare the distributions for the forward and reversed processes. Even though no exact detailed fluctuation theorem is observed for the studied quantity in the absence of detailed balance, we show that the fluctuation ratios (FRs) display intriguing signatures due to the specific dy-

 

TABLE I. The different reaction schemes discussed in this work. Whereas model 1 is an equilibrium model, in models 2, 3, and 4 microscopic reversibility is partly or fully broken. In the modified models 2′, 3′, and 4′, we allow for reversible reactions with rates $\varepsilon_h h$ and $\varepsilon_\lambda \lambda$, with $0<\varepsilon_h \leq 1$ and $0<\varepsilon_\lambda \leq 1$.

| Model 1 | Model 2 | Model 3 | Model 4 |
|---|---|---|---|
| $A+A \xrightarrow{\lambda} 0+A$ | $A+A \xrightarrow{\lambda} 0+A$ | $A+A \xrightarrow{\lambda} 0+0$ | $A+A+A \xrightarrow{\lambda} 0+0+0$ |
| $A+0 \xrightarrow{h} A+A$ | $0 \xrightarrow{h} A$ | $0 \xrightarrow{h} A$ | $0 \xrightarrow{h} A$ |
| | Model 2′ | Model 3′ | Model 4′ |
| | $A+A \underset{\varepsilon_\lambda \lambda}{\overset{\lambda}{\rightleftarrows}} 0+A$ | $A+A \underset{\varepsilon_\lambda \lambda}{\overset{\lambda}{\rightleftarrows}} 0+0$ | $A+A+A \underset{\varepsilon_\lambda \lambda}{\overset{\lambda}{\rightleftarrows}} 0+0+0$ |
| | $0 \underset{\varepsilon_h h}{\overset{h}{\rightleftarrows}} A$ | $0 \underset{\varepsilon_h h}{\overset{h}{\rightleftarrows}} A$ | $0 \underset{\varepsilon_h h}{\overset{h}{\rightleftarrows}} A$ |

namics of the nonequilibrium systems under investigation.

A brief account of some of our results has been given previously [36]. In the present paper, we not only give a detailed study of the features observed in the ratio of the probability distributions for our observable, we also extend our investigation to other reaction schemes not studied previously. This allows us to gain a better understanding of fluctuations in truly nonequilibrium systems driven away from stationarity and to make the discussion in [36] more quantitative.

Our paper is organized in the following way. In the next section, we introduce the different reaction-diffusion models and discuss their steady-state properties. In Sec. III, we drive these systems out of stationarity through time-dependent reaction rates. Using an observable that remains well defined even in the absence of microscopic reversibility, we study the probability distributions for this variable and show that the fluctuation ratios formed by the probability distributions computed in the forward and the reversed processes display features which can be related to the dynamical properties of the nonequilibrium system. Finally, Sec. IV gives our summary as well as an outlook on open problems.

## II. MODELS AND THEIR STEADY-STATE PROPERTIES

We consider one-dimensional lattices made up of $L$ sites with periodic boundary conditions, where every lattice site can at most be occupied by one particle. Because of the exclusion of multiple occupancy of the lattice sites, a total of $2^L$ configurations exist. Particles are allowed to jump to unoccupied nearest-neighbor sites with a diffusion rate $D$ and undergo various creation and annihilation reactions. We discuss in the following four basic reaction schemes (see Table I), and we denote with models 1, 2, 3, and 4 the four models that result from these reaction schemes. In all four models, we have an annihilation process, that takes place with rate $\lambda$, as well as a creation process, where a new particle is created with rate $h$. The different models differ by the way creation and annihilation take place. Let us first discuss the annihilation process. In models 1 and 2, two particles on neighboring sites undergo a reaction, which leads to the destruction of one of the particles. This is different in model 3, where both particles are destroyed at the same time. Finally, in model 4 three neighboring particles are destroyed in the annihilation reaction. For the creation process, we note that whereas in models 2, 3, and 4 new particles are spontaneously created at empty sites, in model 1 a new particle can only be created at an empty site if one of the neighboring sites is already occupied.

These creation and annihilation processes have been chosen in such a way that the models present different degrees of microscopic reversibility. Thus, in model 1 all reactions are reversible, and it is easy to see that this model is in chemical equilibrium for fixed values of the reaction and diffusion rates. Indeed, if both $\lambda$ and $h$ are different from zero, the reaction scheme reduces to a unique reversible reaction and detailed balance is fulfilled. Model 2, on the other hand, does allow for some reactions to be irreversible. For example, a new particle can be created in the middle of two empty sites $000 \rightarrow 0A0$, with rate $h$, but it is not possible to go back immediately to three empty sites, as the newly created particle needs a neighbor for the annihilation process to take place. Finally, all reactions are irreversible in models 3 and 4, yielding a complete absence of microscopic reversibility.

We also studied variants of model 2, 3, and 4 called 2′, 3′, and 4′, where we restore microscopic reversibility by allowing the reversed processes to take place with rates $\varepsilon_h h$ and $\varepsilon_\lambda \lambda$, where $0<\varepsilon_h, \varepsilon_\lambda \leq 1$. Even though all reactions are now reversible, these models do not fulfill detailed balance for $\varepsilon_h, \varepsilon_\lambda < 1$ and are therefore still nonequilibrium models.

For all our models, the dynamics is described by a discrete-time master equation for the probability $P(C_i,t)$ that the system is in configuration $C_i$ at time $t$ [37]

$$P(C_i,t+1) - P(C_i,t) = \sum_j [\omega(C_j \rightarrow C_i)P(C_j,t) - \omega(C_i \rightarrow C_j)P(C_i,t)]. \quad (1)$$

Zia and Schmittmann [38,39] pointed out that for this type of systems, a nonequilibrium steady state is characterized by both the stationary probability distribution $P_s(C_i)$ and the stationary probability currents

$$K^*(C_i,C_j) = \omega(C_j \rightarrow C_i)P_s(C_j) - \omega(C_i \rightarrow C_j)P_s(C_i) \quad (2)$$

between two configurations $C_i$ and $C_j$.

The stationary probabilities are readily obtained for fixed reaction and diffusion rates by setting up the transition-probability matrix $\mathbf{W}$, whose elements are the transition rates between different configurations. Of course, as we have $2^L$ configurations for a system of size $L$, the transition-probability matrix is a $2^L \times 2^L$ matrix. The stationary probabilities are then obtained as the elements of the null eigenvector of the Liouville matrix $\mathbf{L}$, which results when subtracting off the identity matrix from the transition-probability matrix. For systems that are small enough, this

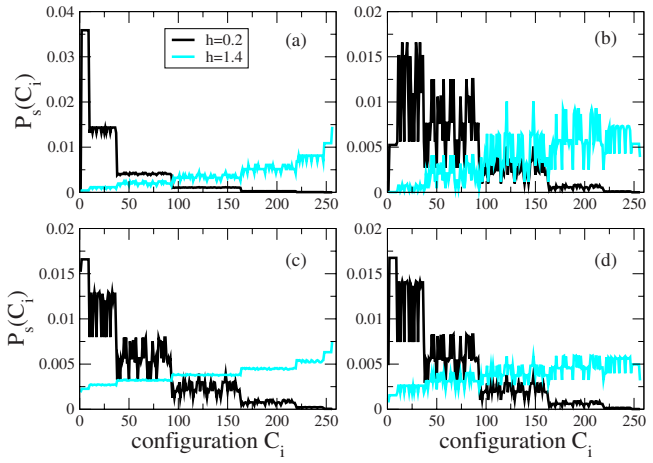


FIG. 1. (Color online) The stationary probabilities for (a) model 1, (b) model 2, and [(c) and (d)] model 3. The common parameter is $\lambda=1$, whereas $D=1$ in (a)–(c) and $D=5$ in (d). The system size is $L=8$. The configurations are grouped by the total number of particles in the system, with the empty configuration on the left and the fully occupied lattice on the right.

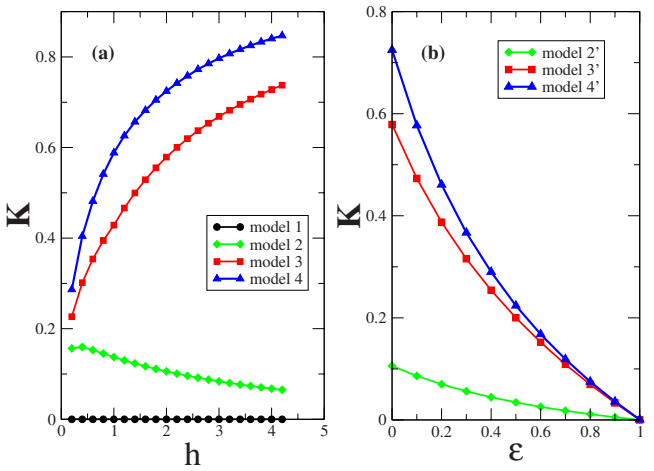


FIG. 2. (Color online) The total probability current $K$ (a) as a function of the creation rate $h$ for models 1, 2, 3, and 4, and (b) as a function of $\varepsilon=\varepsilon_\lambda=\varepsilon_h$ for models 2′, 3′, and 4′. In all cases, $\lambda=1$ and $D=1$. In (b), the creation rate is $h=2$. The data are for systems with $L=8$ lattice sites.

eigenvalue problem can be solved using standard algorithms. For larger system sizes, the stationary probabilities can be measured through standard Monte Carlo simulations.

We show in Fig. 1 the stationary probability distributions for some of the models and various values of the reaction rates. Configurations with the same number of particles are grouped together, with the empty configuration to the left and the fully occupied lattice to the right. The first thing to note is that a change in reaction rates has a large impact on the stationary probability distributions. When the creation of new particles takes place with a small rate (see the black lines in Fig. 1), configurations with only few particles are the most likely. This is different when the creation rate is large, as then configurations with a large number of occupied sites have an increasing weight [see the cyan (light gray) lines in Fig. 1]. A corresponding behavior is observed when changing the rate $\lambda$. On the other hand, however, a change in the value of the diffusion constant $D$ mainly changes the distributions quantitatively [see Figs. 1(c) and 1(d)].

Even though there are visible differences in the stationary probability distributions between Figs. 1(a) and 1(c), it is not possible to guess from these stationary probabilities alone whether the system is in equilibrium, as it is the case for model 1, or whether we are dealing with a nonequilibrium system with a fully irreversible reaction scheme, as for model 3. The stationary probability distribution does not allow by itself to characterize unequivocally nonequilibrium steady states.

Instead of analyzing one by one the stationary probability currents for various configuration pairs, it is more convenient to look at the global quantity [40]

$$K = \sum_{i,j;i<j} |K^*(C_i,C_j)|. \tag{3}$$

In Fig. 2(a), we show the dependence of $K$ on the value of the creation rate $h$ for fixed values of $\lambda$ and $D$. Obviously, the dependence is very different for the different models. In the equilibrium model 1, one does not have any nonvanishing stationary probability currents, and $K$ is zero for all values of the reaction and diffusion rates, as expected. This is different for the nonequilibrium systems, which are characterized by nonvanishing stationary probability currents. Interestingly, the value of $K$ decreases in model 2 for larger $h$, whereas for models 3 and 4 it increases as a function of $h$. In order to understand this difference in behavior, we recall that for larger values of $h$ configurations with a large number of particles have an increased stationary probability. As a result, free sites will have with high probability occupied neighboring sites, and the creation process $0\rightarrow A$ effectively equals the process $A\rightarrow 2A$. This is, however, exactly the reversed reaction to the annihilation process of model 2, which explains why for large $h$ the behavior of model 2 approaches that of an equilibrium system. For models 3 and 4, however, all reactions remain irreversible and $K$ keeps on growing.

In Fig. 2(b), we plot $K$ as a function of the parameter $\varepsilon=\varepsilon_\lambda=\varepsilon_h$ for the modified models 2′, 3′, and 4′ for which we allow the reversed reactions to take place. As a result, all reactions are now reversible, but for all cases we are still out of equilibrium as long as $\varepsilon<1$. Increasing $\varepsilon$ decreases the distance to equilibrium, which is finally reached for $\varepsilon=1$ when all reactions and the corresponding reversed reactions are taking place with the same rate.

This discussion of the stationary probability distributions and of the stationary probability currents shows that it is not possible to characterize in an unambiguous way a nonequilibrium system solely through its stationary probability distribution. Much information is contained in the stationary probability currents, which do allow to distinguish between the properties of equilibrium, weakly nonequilibrium, and strongly nonequilibrium systems. Therefore, these currents allow to quantify the distance to equilibrium, making them a useful tool for the characterization of nonequilibrium systems.

## III. TRANSIENT FLUCTUATION RELATIONS

Having discussed the steady-state properties of reaction-diffusion models, we now focus on the characterization of the transient behavior when the systems are brought out of stationarity and are then allowed to relax to a new steady state. We are realizing this through a protocol in which we change one of the reaction rates. Experimentally, a change in rates of chemical reactions can be achieved by changing the temperature, for example. In our protocol, we change one of the rates $r$ from an initial value $r_0$ to a final value $r_M$ in $M$ equidistant steps of length $\Delta r$, yielding for the reaction rate the values $r_i = r_0 + i\Delta r$ with $i = 0, \ldots, M$. We assume that at every step, only one reaction or diffusion process takes place.

In the following, we discuss mainly numerical exact results for small one-dimensional systems. This numerical exact approach is rather straightforward and is summarized in the Appendix. Larger systems can be studied along the same lines through numerical simulations, but this must be done with some care in order to guarantee a sufficient sampling of rare events [41].

### A. Observables

We discuss in the following two observables, which differ by the fact that for one of the variables microscopic reversibility has to be assumed, whereas for the other no such assumption has to be made. For a system that is microscopic reversible, as, for example, a system that fulfills detailed balance, we will discuss the difference between these two quantities explicitly.

In order to define these quantities, let us first suppose that the system is in a steady state. Starting from a configuration $C_0$, the system is in the configuration $C_i$ at step $i$, such that after $M$ steps the system has performed the following path in configuration state $\mathbf{X} = C_0 \to C_1 \to \cdots \to C_{M-1} \to C_M$. The probability for this path is

$$P(\mathbf{X}) = P_s(C_0) \prod_{i=0}^{M-1} \omega(C_i \to C_{i+1}), \tag{4}$$

where $\omega(C_i \to C_{i+1})$ is the transition probability from configuration $C_i$ to configuration $C_{i+1}$. Denoting the reversed path by $\tilde{\mathbf{X}} = C_M \to C_{M-1} \to \cdots \to C_1 \to C_0$, one then defines for Markovian systems the quantity [8,30]

$$R_{ss} = \ln \frac{P(\mathbf{X})}{P(\tilde{\mathbf{X}})} = \ln \frac{P_s(C_0)}{P_s(C_M)} + \sum_{i=0}^{M-1} \ln \frac{\omega(C_i \to C_{i+1})}{\omega(C_{i+1} \to C_i)}. \tag{5}$$

When the system is driven out of stationarity, we can generalize this definition to a time-dependent reaction rate, yielding

$$R = \ln \frac{P_s(C_0, r_0)}{P_s(C_M, r_M)} + \sum_{i=0}^{M-1} \ln \frac{\omega(C_i \to C_{i+1}, r_{i+1})}{\omega(C_{i+1} \to C_i, r_i)}, \tag{6}$$

where $P_s(C_i, r_i)$ is the probability to find the configuration $C_i$ in the stationary state, corresponding to the value $r_i$ of the reaction rate $r$, and $\omega(C_i \to C_{i+1}, r_{i+1})$ is the transition probability from $C_i$ to $C_{i+1}$ at step $i+1$.

A closer look at the observable $R$ reveals that its definition requires that if $\omega(C_i \to C_{i+1}, r_{i+1}) > 0$ than $\omega(C_{i+1} \to C_i, r_i)$ also has to be nonzero. However, in some of our reaction-diffusion models, this condition is not fulfilled as microscopic reversibility is broken, and we cannot use $R$ to study them. Hatano and Sasa [12] proposed a different quantity that is closely related to $R$ but that does not assume microscopic reversibility. Adapting this quantity for systems driven out of stationarity [42], we can write it in the following way [36]:

$$\phi = \sum_{i=0}^{M-1} \ln \left[ \frac{P_s(C_i, r_i)}{P_s(C_i, r_{i+1})} \right]. \tag{7}$$

The quantity $\phi$ has been called the driving entropy production in [42].

For a system with microscopic reversibility, we can derive a relation between $R$ and $\phi$. With the help of the probability current

$$K^*(C_i, C_{i+1}, r_{i+1}) = \omega(C_{i+1} \to C_i, r_{i+1}) P_s(C_{i+1}, r_{i+1}) - \omega(C_i \to C_{i+1}, r_{i+1}) P_s(C_i, r_{i+1}), \tag{8}$$

we can write Eq. (7) for $\phi$ in the following form:

$$\phi = R - \sum_{i=0}^{M-1} \ln \left[ - \frac{K^*(C_i, C_{i+1}, r_{i+1})}{P_s(C_{i+1}, r_{i+1}) \omega(C_{i+1} \to C_i, r_i)} + \frac{\omega(C_{i+1} \to C_i, r_{i+1})}{\omega(C_{i+1} \to C_i, r_i)} \right], \tag{9}$$

which reveals that the difference between $R$ and $\phi$ is composed of terms which have very different physical origins. The first term in the ln in Eq. (9) is due to nonvanishing probability currents between different configurations and is therefore characteristic for nonequilibrium states. The second term is nontrivial only in transient processes as it accounts for a shift in the reversed transition probability. This term reduces to the trivial value 1 in case one remains in a given steady state, with $r_{i+1} = r_i = r_0$ for all $i$. If this steady state is, in addition, an equilibrium state, the probability currents are all vanishing, and one has $R = \phi = 0$.

It is easy to show [12,14,42] that for transient processes, both quantities fulfill an integral fluctuation theorem $\langle e^{-R} \rangle = 1$ and $\langle e^{-\phi} \rangle = 1$, where the average is taken over all possible histories when driving the system out of a general steady state. For a system that is initially in an equilibrium steady state, the relation $\langle e^{-\phi} \rangle = 1$ reduces to the Jarzynski relation [4] as then $\phi = \beta(W - \Delta F)$, where $W$ is the work done on the system, $\Delta F$ is the free-energy difference between initial and final states, and $\beta$ is the inverse temperature. The difference $W_d = W - \Delta F$ is the dissipative work.

### B. Probability distributions

In systems with detailed balance, an exact fluctuation relation is obtained when plotting the ratio between the probability distributions $P_F(\beta W_d)$ and $P_R(-\beta W_d)$ of the dissipative work $W_d$ done on the system in the forward and reversed processes [10],

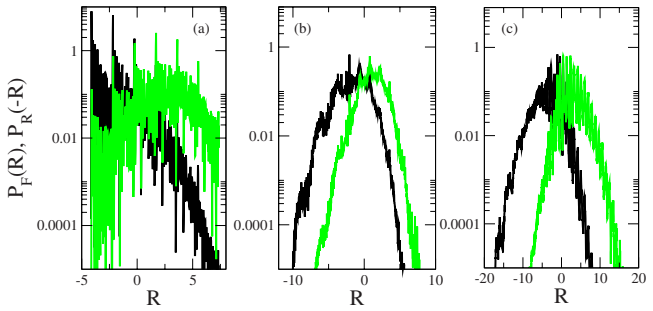


FIG. 3. (Color online) Probability distributions for the quantity $R$ when the creation rate is changed in $M=6$ equidistant steps from 0.2 to 1.4 [$P_F(R)$, black curve] or from 1.4 to 0.2 [$P_R(-R)$, green (gray) curve]. The data have been obtained for a system with $L=8$ sites, with $D=5$ and $\lambda=1$. (a) Model 1, (b) model 2′ with $\varepsilon=0.1$, and (c) model 3′ with $\varepsilon=0.1$.

$$\frac{P_F(\beta W_d)}{P_R(-\beta W_d)} = e^{\beta W_d}. \tag{10}$$

Recalling that for systems with detailed balance, we have the identity $\phi=W_d$, it is tempting to ask whether for $\phi$ an exact fluctuation theorem, such as Eq. (10), can also be encountered for a system initially in a nonequilibrium steady state. In fact, this is not the case: the absence of detailed balance in a nonequilibrium steady state entails nonzero probability currents, and no simple relation, such as the relation (10), exists for $\phi$ in this case. As we shall discuss below, the corresponding fluctuation ratios yield *systematic* deviations from the simple behavior encountered in systems with detailed balance, these deviations containing nontrivial information on the nonequilibrium system at hand.

However, before analyzing these ratios of probability distributions, we shall first discuss the probability distributions themselves.

Figures 3–6 show typical examples for the probability distributions of $R$ and $\phi$ when changing the creation rate from an initial value $h_0$ to a final value $h_M$ in $M$ steps (we only show the case of a varying creation rate $h$, but the following discussion can be made along similar lines when changing the value of the annihilation rate $\lambda$).

Figure 3 shows the probability distributions of $R$ for three cases that fulfill microscopic reversibility: models 1, 2′, and 3′. These different probability distributions are not Gaussian

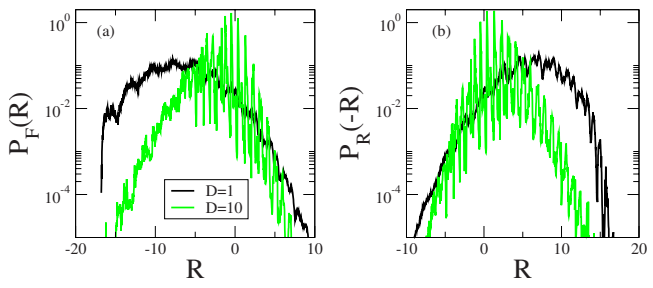


FIG. 4. (Color online) The same as in Fig. 3, but now for model 3′ and two different values of the diffusion rate. (a) $P_F(R)$ from the forward process and (b) $P_R(-R)$ from the reversed process.

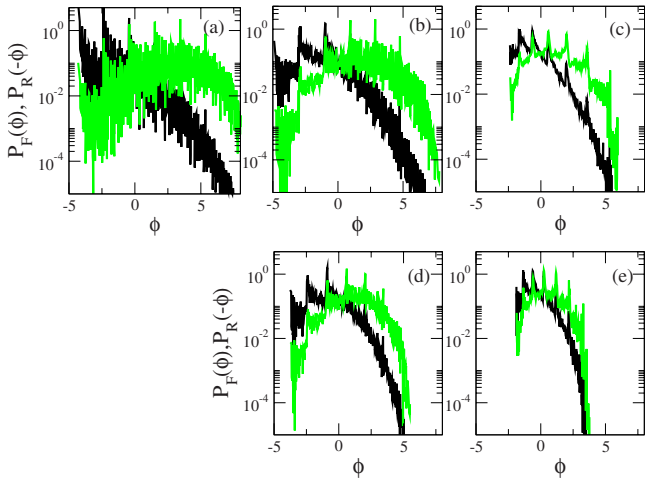


FIG. 5. (Color online) Probability distributions for the quantity $\phi$ when the creation rate $h$ is changed in $M=6$ steps from 0.2 to 1.4 [$P_F(\phi)$, black curve] or from 1.4 to 0.2 [$P_R(-\phi)$, green (gray) curve]. The data have been obtained for a system with $L=8$ sites, with $D=5$ and $\lambda=1$. (a) Model 1, (b) model 2, (c) model 3, (d) model 2′ with $\varepsilon=0.1$, and (e) model 3′ with $\varepsilon=0.1$.

but are characterized by a rather irregular structure. Their shape depends on the dynamics of the different models expressed by the different reaction schemes. It is, however, not straightforward to relate specific features of the probability distributions to the different reactions. It is important to note that the peaks dominating these distributions do not have their origin in the noisiness of some numerical data but are real as we are using a numerically exact method. In addition,

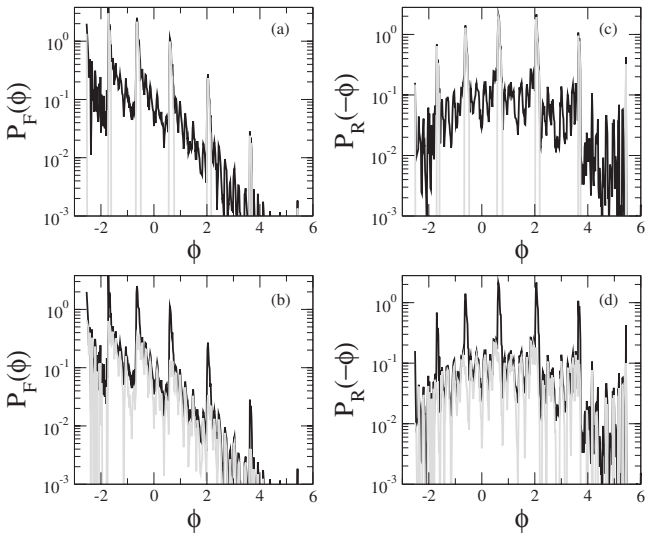


FIG. 6. Main contributions to the probability distributions for $\phi$ in the forward and reversed processes. The black lines show the full probability distributions, whereas the gray lines show the contributions coming from [(a) and (c)] trajectories in configuration space with only diffusion steps and no reactions and [(b) and (d)] from trajectories, where exactly one reaction takes place that changes the number of particles in the system. The data are for model 3 with $D=10$, $h_0=0.2$, $\Delta h=1.2$, and $\lambda=1$. The system size is $L=8$ and the driving length is $M=6$.

our numerically exact method also allows us to circumvent any issues that might appear due to an insufficient sampling of rare events. This will be of importance in the next section when we discuss the ratios of the forward and reversed probability distributions.

The probability distributions show a strong dependence on the system parameters. This is illustrated in Fig. 4, where we compare for model 3′ the distributions obtained for different values of the diffusion rate. When we increase the diffusion rate, the general shape of the probability distribution changes and, in addition, a large number of distinct peaks appear.

The probability distributions for $\phi$ differ markedly from those for $R$ (see Fig. 5). This was expected as the main differences between both quantities are the probability currents, which are nonzero for a system that is out of equilibrium. It is only for the equilibrium model 1 that the distributions for both quantities are similar. Interestingly, the probability distributions for $\phi$ for both the forward and reversed processes are characterized by the presence of prominent peaks. An increase in the diffusion constant strongly amplifies these peaks but does not change the overall shape of the probability distributions. The fact that the heights of the peaks depend on the value of the diffusion constant indicates that these peaks are related to trajectories in configuration space that are dominated by diffusion steps and not by reactions. In Fig. 6, we verify for model 3 that the main contributions to the peaks for a drive of length $M=6$ indeed come from the trajectories, where only diffusion takes place such that the number of particles is constant along these trajectories. The subleading contribution, also shown in Fig. 6, comes from the trajectories where a single reaction takes place, which changes the number of particles in the system. Because the peaks are dominated by trajectories with pure diffusion, the positions of the peaks are the same for the forward and reversed processes, the leftmost peak resulting from the diffusion of a single particle in the system, whereas the rightmost peak is due to the diffusion of a single empty site in the system.

Before closing this section, we remark that in [42] similar peaks have been observed in the probability distributions of the driving entropy production as well as of other related quantities in a model for electron transport through a single level quantum dot.

### C. Fluctuation ratios

Having just discussed the probability distributions of the quantities $R$ and $\phi$, we now move on and study the fluctuation ratios formed by these probability distributions. For a system driven out of an initial equilibrium state and fulfilling detailed balance, Crooks showed the exact relation (10) to exist between the probability distributions of the dissipative work measured in the forward and time-reversed processes. This remarkable result can be extended to systems that are still reversible microscopically but that do not fulfill detailed balance any more [16]. As illustrated in Fig. 7 for models 2′ and 3′, the ratios of the probability distributions for $R$ show a simple exponential dependence on $R$. The perfect exponential obtained from our data nicely validates our numerical exact approach. Obtaining a plot of similar quality through Monte Carlo simulations is difficult as rare events are then hard to measure.

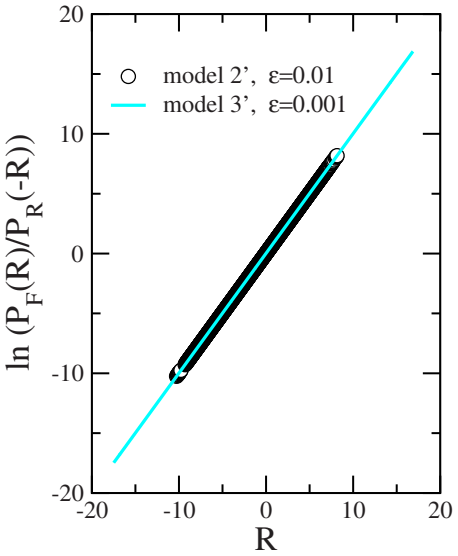


FIG. 7. (Color online) Fluctuation relation for the observable $R$ for model 2′ and model 3′ for different values of the parameter $\varepsilon$. The parameters in this calculation are $h_0=0.2$, $\Delta h=1.2$, $\lambda=1$, and $D=5$. The system size is $L=8$ and the driving length is $M=6$.

Even though in the absence of microscopic reversibility $R$ is ill defined, this is different for $\phi$ as this quantity exclusively involves the steady-state probabilities [see Eq. (7)]. For an equilibrium system, $\phi$ fulfills an exact fluctuation theorem as it then reduces exactly to the dissipative work. As shown in Fig. 8 for model 1, an exponential relation is indeed obtained for all parameter values as well as for different driving processes $h(t)$.

However, for a system with nonequilibrium steady states, no exponential detailed fluctuation relation is expected for $\phi$

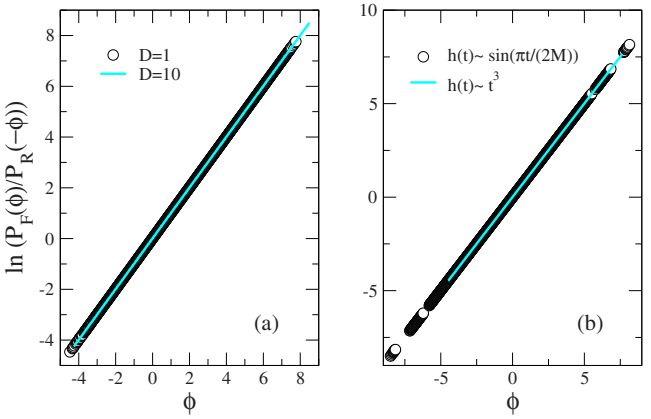


FIG. 8. (Color online) Fluctuation relation for the observable $\phi$ for model 1 with (a) different values of $D$ and (b) different ways of changing the parameter $h(t)$ with $D=1$. The driving process usually studied in this paper and which yields the data shown in (a) is $h(t)\sim t$. The parameters used in these calculations are $h_0=0.2$, $\Delta h=1.2$, and $\lambda=1$. The system size is $L=8$ and the driving length is $M=6$.

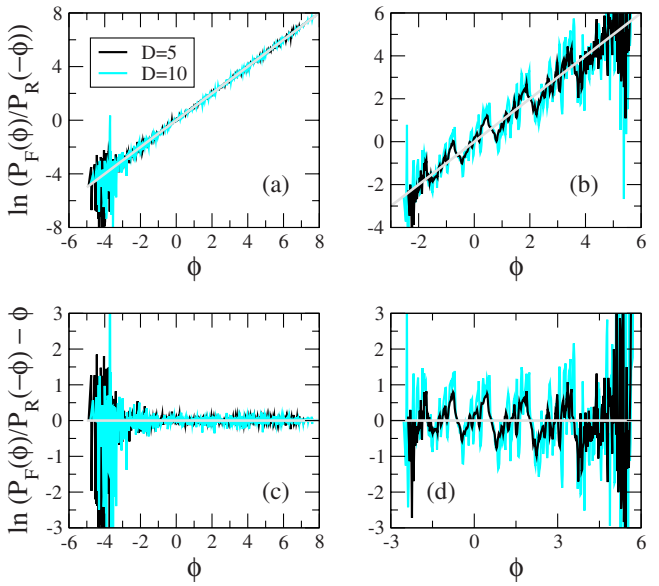


FIG. 9. (Color online) Fluctuation ratios for the observable $\phi$ for (a) model 2 and (b) model 3 and different values of the diffusion constant $D$. Whereas in model 2 only random deviations from a simple exponential behavior are observed, systematic deviations show up for model 3. This is highlighted in (c) and (d), where we subtract $\phi$ from the logarithm of the fluctuation ratio. The light gray lines indicate a simple exponential dependence. The parameters used in this calculation are $h_0=0.2$, $\Delta h=1.2$, and $\lambda=1$. The system size is $L=8$ and the driving length is $M=6$.

as this quantity does not contain the information on nonequilibrium currents [see Eq. (9)]. We show in Fig. 9 ratios of the probability distributions of $\phi$ for models 2 and 3. For model 2, the deviations from the exponential are random and no pronounced dependence on system parameters, as, for example, the diffusion rate $D$, is observed. For model 3, however, a qualitatively different behavior is encountered and *systematic* deviations in the form of oscillations are observed. Similar oscillations are also observed for model 4, where three neighboring particles are destroyed in the annihilation process. Interestingly, the amplitudes of these oscillations increase for increasing diffusion rates. At first, one might think that this increase in peak height when increasing $D$ should be related to the increase in the peaks in the probability distributions themselves (see the discussion in the previous section). However, this is too simplistic as an increase in peak heights in the probability distributions is also observed for models 1 and 2, for which we do not observe the corresponding behavior in the fluctuation ratios. What is different between models 1 and 2, on one hand, and models 3 and 4, on the other hand, is that for the former models any change in the forward and reversed probability distributions is compensated when forming the ratio (this compensation is exact for model 1 and approximate for model 2), whereas for the latter models this compensation is only partial, such giving rise to peaks also in the fluctuation ratios.

Before discussing the origin of this difference, let us first have for model 3 a closer look at the peaks in the fluctuation ratio. We first note that the positions of these peaks are *not* identical to the positions of the extrema in the probability distributions (see, for example, Fig. 6). In Table II, we compare the positions of the maxima and minima in the fluctuation ratio with the peak positions in the probability distributions. The observed offset means that the peaks in the probability distributions for the forward and reversed processes compensate each other when forming the ratio but that the compensation is only partial away from the peaks. Recalling that the peaks result from trajectories in configuration space with only diffusion steps and that trajectories with reactions make up the part between the peaks, we can conclude that reactions are responsible for the peaks in the fluctuation ratios. In order to verify this assumption, we analyzed the contributions to the fluctuation ratio coming from the different types of trajectories. We show in Fig. 10 that the observed minima and maxima are indeed mainly due to the trajectories with a single reaction process. For this, we compare the fluctuation ratio with the quantity $\Pi_F(\phi)/\Pi_R(-\phi)$, where $\Pi(\phi)$ is the probability distribution for all trajectories having (a) only diffusion steps or (b) exactly one reaction process. Obviously, the peaks in the latter ratio coincide with the peaks in the fluctuation ratio.

TABLE II. Positions of the maxima in the PDs and of the maxima and minima in the FR for model 3, with $D=5$, $h_0=0.2$, $\Delta h=1.2$, and $\lambda=1$. The system size is $L=8$ and the driving length is $M=6$.

| PD maxima | FR maxima | FR minima |
|---|---|---|
| −1.63 | −1.78 | −1.5 |
| −0.61 | −0.72 | −0.38 |
| 0.60 | 0.50 | 0.82 |
| 2.02 | 1.89 | 2.25 |
| 3.64 | 3.44 | 3.84 |

As a second interesting observation, we note that the oscillations in the fluctuation ratios are not restricted to cases

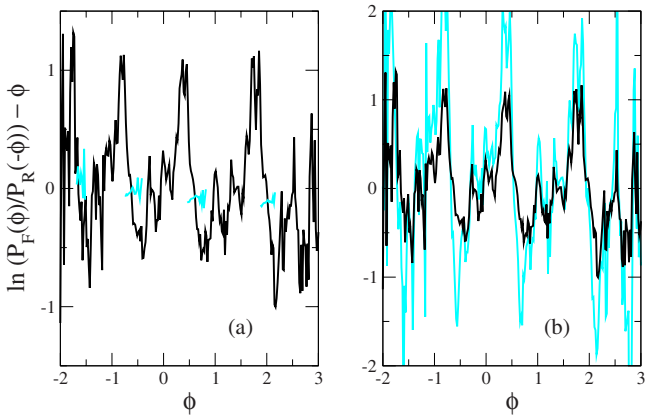


FIG. 10. (Color online) Comparison for model 3 of the fluctuation ratio (black line) with the ratio $\Pi_F(\phi)/\Pi_R(-\phi)$ [cyan (light gray) line], where $\Pi(\phi)$ is the probability distribution of $\phi$ for all trajectories with (a) only diffusion steps and (b) exactly one reaction process. Note that for trajectories with only diffusion, few values of $\phi$ can be realized. The common parameters are $h=0.2$, $\lambda=1.$, $M=6$ and $L=8$, and $D=5$.

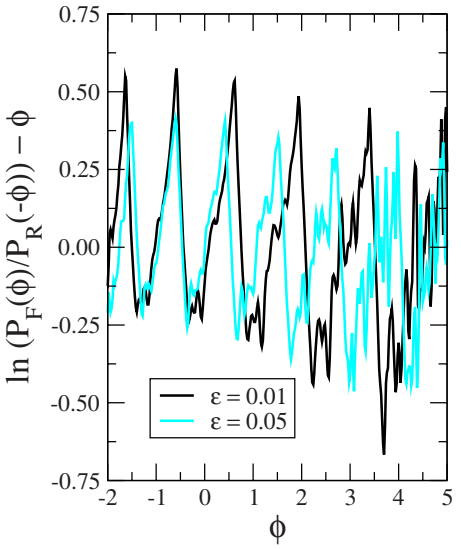


FIG. 11. (Color online) Fluctuation relations for model 3′ and different values of $\varepsilon$. The values of the parameters are $D=5$, $h_0=0.2$, $\Delta h=1.2$, and $\lambda=1$. The system size here is $L=10$ and the driving length is $M=10$. These data have been obtained through Monte Carlo simulations.

where microscopic reversibility is broken but are much more widespread. As is shown in Fig. 11 for model 3′ (the same holds for model 4′), peaks in the fluctuation ratios also show up in some systems where all reactions are reversible.

In order to understand the origin of these oscillations, we need to go back to the different reaction schemes summarized in Table I. The configuration space of a reaction-diffusion system can be thought to be composed of smaller units formed by the configurations with a common number $N$ of particles. A diffusion step conserves the number of particles, thereby, connecting two configurations in the same unit. A passage from one unit to another always involves a change in particle number and is therefore exclusively due to a reaction process. This is sketched in Fig. 12. Keeping this in mind, a fundamental difference emerges between models 1 and 2, on one hand, and models 3 and 4, on the other hand. In the former systems, every reaction changes the particle number by 1, $\Delta N=\pm 1$. In the latter systems, however, also larger changes in the particle number happen in the annihilation process, with $\Delta N=-2$ for model 3 and $\Delta N=-3$ for model 4. As a consequence, loops in configuration space that connect a unit with constant $N$ with itself and that involve reactions will display an asymmetry in the number of creation and annihilation processes. Thus, for model 3 the smallest loop contains two creation processes and one annihilation. This effect is still present, even though in a weaker form, when we add the backreactions and end up with a microscopically reversible model, such as model 3′, with a variable number of particles added or subtracted in the different reactions. It is this difference in the number of particles created in a creation process or destroyed in an annihilation event that yields contributions to the probability distributions, which are not compensated in the fluctuation ratio.

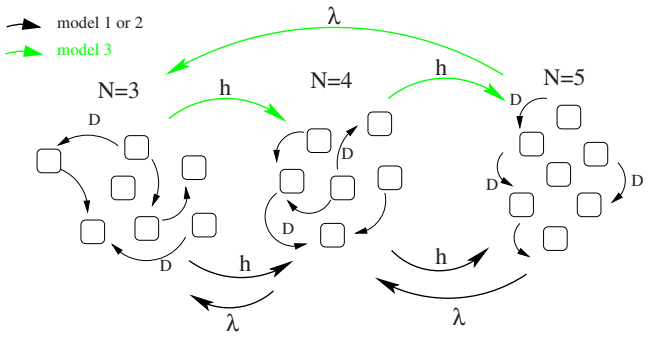


FIG. 12. (Color online) Schematic plot of the configuration space for models 1, 2, and 3, where configurations are grouped by the number of particles in the system $N$. In a diffusion step, the system goes from one configuration to another in the same unit without changing the particle number. Passages between different units are due to reaction processes. For models 1 and 2, one always has that $\Delta N=\pm 1$. This is different for model 3 (and 4), where different reactions yield different changes in the number of particles in the system.

## IV. DISCUSSION

Characterizing the out-of-equilibrium properties of interacting many-body systems remains one of the most challenging tasks in contemporary physics. The recent advent of exact fluctuation and work theorems yielded some excitement in the community as it indicated a possible way of characterizing large classes of nonequilibrium systems.

In our work, we try to characterize diffusion-limited reactions both in their nonequilibrium steady state and in the transient state when the systems are driven out of stationarity. For systems in their steady state, we confirm the expectation that probability currents allow to distinguish between equilibrium and nonequilibrium steady states. In addition, they also allow to define a global quantity that quantifies the distance to equilibrium. This way of characterizing nonequilibrium steady systems remains valid even when microscopic reversibility is broken, as it is the case for many reaction-diffusion systems.

The situation is more complicated if one wishes to characterize reaction-diffusion systems through fluctuation and work theorems. If one studies a system for which microscopic reversibility is fulfilled, one can define a worklike quantity, our quantity $R$ [see Eq. (6)], for which exact detailed fluctuation theorems not only hold in the steady states but are also valid when the system is driven out of stationarity through time-dependent reaction rates. In the absence of microscopic reversibility, however, $R$ cannot be used as it is no longer well defined. Instead, we propose to use the driving entropy production $\phi$ [see Eq. (7)], initially introduced in [12,42], as this quantity exclusively uses stationary probabilities and therefore remains well defined even in the absence of microscopic reversibility. Whereas the driving entropy production always fulfills a global fluctuation theorem [12,42], it only fulfills a detailed fluctuation theorem for systems with equilibrium steady states. At first look, this seems to strongly reduce the usefulness of his quantity for the characterization of systems with nonequilibrium steady states.

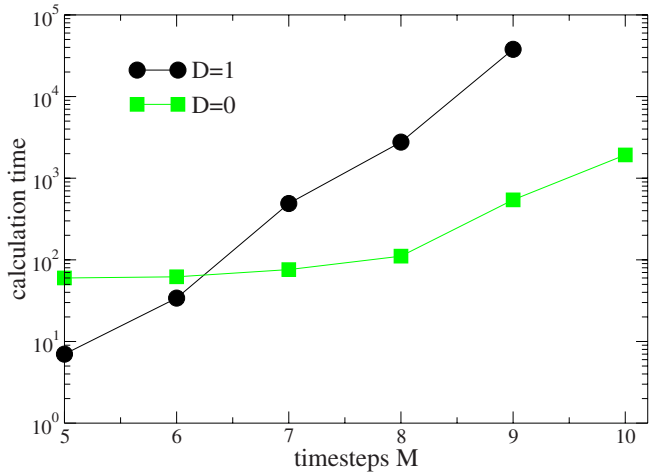


FIG. 13. (Color online) Exponential growth of the calculation time in function of the number of steps for model 1 with $L=6$ sites, where the creation rate $h$ was changed between $h_0=0.2$ and $h_M=1.4$. For this calculation, we set $\lambda=1.0$ and considered both vanishing ($D=0$) and nonvanishing ($D=1$) diffusion rates.

However, as we showed in this paper, the deviations of the fluctuation ratios for $\phi$ from a simple exponential behavior do contain nontrivial information on the trajectories in configuration space. Indeed, in cases where the change in the number of particles is different for different reactions, we observe systematic deviations from a simple exponential behavior. These deviations, which take the form of peaks superimposed on an exponential, mainly result from trajectories in configuration space, where exactly one reaction takes place.

It is not an easy task to quantitatively relate the peak heights and the peak positions to the values of the system parameters. For this, a much more in-depth study is needed, where all the parameters are varied in a systematic way [41].

Whereas the driving entropy production $\phi$ remains a well-defined quantity even in the absence of microscopic reversibility, we need to mention that in many cases this could be a quantity that is difficult to measure as the knowledge of the stationary probability distribution of the system is required. As a consequence, the practical importance of $\phi$ could be restricted, especially for experimental systems where the stationary probability distribution is often not easily accessible.

How general are the results found in this work? Based on the reaction schemes discussed in this work and given in Table I, we expect the peaks to appear in the fluctuation ratios for $\phi$ for any reaction-diffusion system that allows for a variable number of particles to be created or destroyed in the different reactions. This also encompasses more complicated systems with two or more particle types. In addition, signatures of the same type should also be observed for other system classes with a configuration-space topology that is similar to that of the reaction-diffusion systems (i.e., composed by groups of configurations that are only connected in a very specific way) and with a similar asymmetry in the configuration-space trajectories. An extension of our work along these lines is planed for the future.


## ACKNOWLEDGMENTS

We thank Chris Jarzynski and Frédéric van Wijland for interesting and stimulating discussions. This work was supported by the U.S. National Science Foundation through Grant No. DMR-0904999.


## APPENDIX

In order to compute the probability distribution of $\phi$ [see Eq. (7)], when changing some rate $r$ from its initial value $r_0$ to the final value $r_M$ in $M$ steps, with $r_i=r_0+\frac{i}{M}(r_M-r_i)$, $i=0,\ldots,M$, we first need to know the stationary probability distributions for any value $r_i$. This is easily done by determining the null eigenvector of the Liouville matrix. We then need to generate all possible sequences of configurations (*paths* in configuration space) $\mathbf{X}=C_0\to C_1\to\cdots\to C_{M-1}\to C_M$, where only one reaction or diffusion takes place at every step. Starting from every possible initial configuration, we have to built up a tree structure to all the configurations that can be reached in $M$ steps with nonzero probability. This is done recursively by a standard depth-first search algorithm that ends when we reach the $M$th step. We now have to attach a probability to every one of these generated paths. For this, we are multiplying the probability to select the initial configuration $C_0$ with the product of the $M$ transition probabilities,

$$P_F(\mathbf{X}) = P_s(C_0,r_0)\prod_{i=0}^{M-1}\omega(C_i\to C_{i+1},r_{i+1}). \tag{A1}$$

Having now determined every path and its probability, we need, in addition, the values of $\phi$ along these different paths, which we obtain through the equation

$$\tilde{\phi}(\mathbf{X}) = \sum_{i=0}^{M-1}[\ln P_s(C_i,r_{i+1}) - \ln P_s(C_i,r_i)], \tag{A2}$$

where $P_s(C_i,r_i)$ is the stationary probability to find the configuration $C_i$ at the value $r_i$ of the rate $r$. Putting everything together, the probability distribution is finally obtained through the expression

$$P_F(\phi) = \sum_{\mathbf{X}} P_F(\mathbf{X})\delta[\tilde{\phi}(\mathbf{X})-\phi]. \tag{A3}$$

In addition to the just-described forward process, we also study the reversed process, where we start in configuration $C_M$ with the rate $r_M$ before changing the reaction rate in $M$ steps to its final value $r_0$. The probability distribution for this process is then

$$P_R(\phi) = \sum_{\tilde{\mathbf{X}}} P_R(\tilde{\mathbf{X}})\delta[\tilde{\phi}(\tilde{\mathbf{X}})-\phi], \tag{A4}$$

with

$$P_R(\tilde{\mathbf{X}}) = P_s(C_M,r_M)\prod_{i=0}^{M-1}\omega(C_{M-i}\to C_{M-1-i},r_{M-1-i}). \tag{A5}$$

In Sec. III, we discuss not only the quantity $\phi$ but also the quantity $R$ defined by Eq. (6). For this second quantity, the procedure is exactly the same, only the calculation of the values of $\phi$ for the different paths has to be replaced by the values of $R$.

This numerical exact approach is limited to small system sizes $L$ and few steps $M$, as the number of paths grows exponentially with both $L$ and $M$ [see Fig. 13]. For example, for $L=6$ the number of paths increases from 404 for $M=2$ to $8.6\times10^8$ for $M=9$.


[1] D. J. Evans, E. G. D. Cohen, and G. P. Morriss, Phys. Rev. Lett. **71**, 2401 (1993).
[2] D. J. Evans and D. J. Searles, Phys. Rev. E **50**, 1645 (1994).
[3] G. Gallavotti and E. G. D. Cohen, Phys. Rev. Lett. **74**, 2694 (1995).
[4] C. Jarzynski, Phys. Rev. Lett. **78**, 2690 (1997).
[5] C. Jarzynski, Phys. Rev. E **56**, 5018 (1997).
[6] J. Kurchan, J. Phys. A **31**, 3719 (1998).
[7] G. E. Crooks, J. Stat. Phys. **90**, 1481 (1998).
[8] J. L. Lebowitz and H. Spohn, J. Stat. Phys. **95**, 333 (1999).
[9] G. E. Crooks, Phys. Rev. E **60**, 2721 (1999).
[10] G. E. Crooks, Phys. Rev. E **61**, 2361 (2000).
[11] C. Jarzynski, J. Stat. Phys. **98**, 77 (2000).
[12] T. Hatano and S.-I. Sasa, Phys. Rev. Lett. **86**, 3463 (2001).
[13] S. Mukamel, Phys. Rev. Lett. **90**, 170604 (2003).
[14] U. Seifert, Phys. Rev. Lett. **95**, 040602 (2005).
[15] T. Speck and U. Seifert, J. Phys. A **38**, L581 (2005).
[16] R. J. Harris and G. M. Schütz, J. Stat. Mech.: Theory Exp. (2007) P07020.
[17] J. Liphardt, S. Dumont, S. B. Smith, I. Tinico, Jr., and C. Bustamante, Science **296**, 1832 (2002).
[18] D. Collin, F. Ritort, C. Jarzynski, S. B. Smith, I. Tinico, Jr., and C. Bustamante, Nature (London) **437**, 231 (2005).
[19] F. Douarche, S. Ciliberto, A. Petrosyan, and I. Rabbiosi, Europhys. Lett. **70**, 593 (2005).
[20] G. M. Wang, E. M. Sevick, E. Mittag, D. J. Searles, and D. J. Evans, Phys. Rev. Lett. **89**, 050601 (2002).
[21] D. M. Carberry, J. C. Reid, G. M. Wang, E. M. Sevick, D. J. Searles, and D. J. Evans, Phys. Rev. Lett. **92**, 140601 (2004).
[22] C. Tietz, S. Schuler, T. Speck, U. Seifert, and J. Wrachtrup, Phys. Rev. Lett. **97**, 050602 (2006).
[23] S. Joubaud, N. B. Garnier, and S. Ciliberto, Europhys. Lett. **82**, 30007 (2008).
[24] J. Berg, Phys. Rev. Lett. **100**, 188101 (2008).
[25] M. Henkel, H. Hinrichsen, and S. Lübeck, *Non-Equilibrium Phase Transitions*, Absorbing Phase Transitions (Springer, Dordrecht/Canopus, Bristol, 2008), Vol. 1.
[26] G. Ódor, *Universality in Nonequilibrium Lattice Systems: Theoretical Foundations* (World Scientific, Singapore, 2008).
[27] P. Gaspard, J. Chem. Phys. **120**, 8898 (2004).
[28] U. Seifert, J. Phys. A **37**, L517 (2004).
[29] D. Andrieux and P. Gaspard, J. Chem. Phys. **121**, 6167 (2004).
[30] U. Seifert, Europhys. Lett. **70**, 36 (2005).
[31] D. Andrieux and P. Gaspard, Phys. Rev. E **74**, 011906 (2006).
[32] T. Schmiedl and U. Seifert, J. Chem. Phys. **126**, 044101 (2007).
[33] D. Andrieux and P. Gaspard, Phys. Rev. E **77**, 031137 (2008).
[34] S. Chong, M. Otsuki, and H. Hayakawa, e-print arXiv:0906.1930.
[35] J. Ohkubo, e-print arXiv:0909.5292.
[36] S. Dorosz and M. Pleimling, Phys. Rev. E **79**, 030102(R) (2009).
[37] P. Gaspard, J. Stat. Phys. **117**, 599 (2004).
[38] R. K. P. Zia and B. Schmittmann, J. Phys. A **39**, L407 (2006).
[39] R. K. P. Zia and B. Schmittmann, J. Stat. Phys. (2007) P07012.
[40] T. Platini and R. K. P. Zia (private communication).
[41] S. Dorosz amd M. Pleimling (unpublished).
[42] M. Esposito, U. Harbola, and S. Mukamel, Phys. Rev. E **76**, 031132 (2007).